

**Molecular Basis of Cell and  
Developmental Biology:  
Wnt-dependent Regulation of the  
E-cadherin Repressor Snail**

Jong In Yook, Xiao-Yan Li, Ichiro Ota, Eric

R. Fearon and Stephen J. Weiss

*J. Biol. Chem.* 2005, 280:11740-11748.

doi: 10.1074/jbc.M413878200 originally published online January 11, 2005

---

Access the most updated version of this article at doi: [10.1074/jbc.M413878200](https://doi.org/10.1074/jbc.M413878200)

Find articles, minireviews, Reflections and Classics on similar topics on the [JBC Affinity Sites](#).

Alerts:

- [When this article is cited](#)
- [When a correction for this article is posted](#)

[Click here](#) to choose from all of JBC's e-mail alerts

This article cites 45 references, 20 of which can be accessed free at  
<http://www.jbc.org/content/280/12/11740.full.html#ref-list-1>

## Wnt-dependent Regulation of the E-cadherin Repressor Snail\*

Received for publication, December 9, 2004, and in revised form, January 5, 2005  
Published, JBC Papers in Press, January 11, 2005, DOI 10.1074/jbc.M413878200

Jong In Yook‡§, Xiao-Yan Li§, Ichiro Ota§, Eric R. Fearon§¶\*\*, and Stephen J. Weiss§\*\*\*‡

From the ‡Department of Oral Pathology, BK21 Project for Medical Science, College of Dentistry, Yonsei University, Seoul 120-742, Korea and the Division of Molecular Medicine & Genetics, Departments of §Internal Medicine, ¶Human Genetics, and ||Pathology and the \*\*University of Michigan Comprehensive Cancer Center, University of Michigan, Ann Arbor, Michigan 48109

**Down-regulation of E-cadherin marks the initiation of the epithelial-mesenchymal transition, a process exploited by invasive cancer cells. The zinc finger transcription factor, Snail, functions as a potent repressor of E-cadherin expression that can, acting alone or in concert with the Wnt/ $\beta$ -catenin/T cell factor axis, induce an epithelial-mesenchymal transition. Although mechanisms that coordinate signaling events initiated by Snail and Wnt remain undefined, we demonstrate that Snail displays  $\beta$ -catenin-like canonical motifs that support its GSK3 $\beta$ -dependent phosphorylation,  $\beta$ -TrCP-directed ubiquitination, and proteasomal degradation. Accordingly, Wnt signaling inhibits Snail phosphorylation and consequently increases Snail protein levels and activity while driving an *in vivo* epithelial-mesenchymal transition that is suppressed following Snail knock-down. These findings define a potential mechanism whereby Wnt signaling stabilizes Snail and  $\beta$ -catenin proteins in tandem fashion so as to cooperatively engage transcriptional programs that control an epithelial-mesenchymal transition.**

E-cadherin, the prototypic member of the cadherin single-pass transmembrane glycoprotein family, regulates cell adhesion in epithelial cells in a  $\text{Ca}^{2+}$ -dependent manner via homotypic interactions with E-cadherin molecules on opposing cell surfaces (1). The adhesive function of E-cadherin is dependent on its binding to the cytoplasmic  $\alpha$ - and  $\beta$ -catenin proteins, which serve to tether the cadherin to the actin cytoskeleton (1). During embryonic development, down-regulation of E-cadherin function marks the onset of a complex program wherein epithelial cells adopt a fibroblast-like phenotype and display tissue invasive activity, a process termed the epithelial-mesenchymal transition (EMT)<sup>1</sup> (1, 2). Likewise, E-cadherin repression is thought to play a major role in the abnormal

manifestation of EMT in epithelial-derived cancer types (3–5). In both development and cancer, the zinc finger transcription factor, Snail, has been implicated in E-cadherin repression via its binding to elements in the E-cadherin promoter (6). Indeed, during development, Snail plays a required role in driving the EMT programs that mark gastrulation as well as neural crest development (1, 3–6). In a similar, but misdirected fashion, neoplastic cells co-opt Snail function to adopt a mesenchymal cell-like invasive phenotype that characterizes their aberrant behavior (1, 3–7).

Although Snail plays a critical role in both physiologic and pathologic EMT (5–8), E-cadherin repression frequently occurs in tandem with activation of the Wnt signaling cascade (9–14). Of note, independent of its well defined role in E-cadherin-dependent adhesion,  $\beta$ -catenin also participates in Wnt signaling (1, 2). In the absence of a Wnt signal, cytosolic  $\beta$ -catenin is normally phosphorylated by glycogen-synthase kinase 3 $\beta$  (GSK3 $\beta$ ) at one or more serine or threonine residues in its N-terminal domain (1, 2). The N-terminally phosphorylated  $\beta$ -catenin is then recognized and ubiquitinated by a multiprotein complex containing the F-box protein  $\beta$ -TrCP, with resultant degradation of the poly-ubiquitinated  $\beta$ -catenin in the proteasome (1, 2). Alternatively, a subset of the 19 known Wnt genes found in mammals (*e.g.* Wnt-1) can activate a pathway that inhibits the ability of GSK3 $\beta$  to phosphorylate target substrates via a process dependent on the protein Dvl (dishevelled) with resultant increases in  $\beta$ -catenin levels (1, 2). The stabilization of  $\beta$ -catenin consequently leads to both enhanced nuclear accumulation and enhanced binding to members of the T cell factor (TCF) family of transcription factors (1, 2). In turn,  $\beta$ -catenin-TCF complexes regulate the expression of a panoply of gene products that direct cell fate, polarity, and proliferation (1, 2).

Although Wnt signaling could conceivably stabilize the pool of cytosolic  $\beta$ -catenin that is released from E-cadherin-bound sites as a consequence of Snail-mediated E-cadherin repression (1, 2, 9), direct interplay between the Wnt and Snail systems has remained a subject of conjecture. Herein, we demonstrate that the Snail transcript encodes a series of  $\beta$ -catenin-like canonical motifs that support its GSK3 $\beta$ -dependent phosphorylation,  $\beta$ -TrCP-directed ubiquitination, and proteasomal degradation via a Wnt-1-regulatable process. Because increasing evidence indicates that Wnt signals can impact on multiple cell functions in neoplastic tissues (12–16), these findings support a model wherein activation of the Wnt-GSK3 $\beta$  signaling cascade regulates carcinoma cell phenotype by controlling  $\beta$ -catenin-TCF- and Snail-dependent transcriptional programs in tandem fashion.

### EXPERIMENTAL PROCEDURES

**Plasmids**—A human Snail cDNA with a C-terminal FLAG (Flg) epitope tag was subcloned into three expression vectors: pCR3.1, to

\* This work was supported by Medical Science and Engineering Research Program of the Korea Science & Engineering Foundation Grant R13-2003-013 (to J. I. Y.), National Institutes of Health Grants R01 CA071699 (to S. J. W.) and R01 CA088308 (to S. J. W.), Komen Foundation Grant BCTR00-000572 (to S. J. W.), and National Institutes of Health Grant R01 CA085463 (to E. R. F.). The costs of publication of this article were defrayed in part by the payment of page charges. This article must therefore be hereby marked “advertisement” in accordance with 18 U.S.C. Section 1734 solely to indicate this fact.

‡ To whom correspondence should be addressed: University of Michigan, 5403 Life Sciences Institute, 210 Washtenaw, Ann Arbor, MI 48109-2216. Tel.: 734-764-0030; Fax: 734-647-7950; E-mail: SJWEISS@umich.edu.

<sup>1</sup> The abbreviations used are: EMT, epithelial-mesenchymal transition; GSK, glycogen-synthase kinase; TCF, T cell factor; HA, hemagglutinin; siRNA, small inhibitory RNA; shRNA, short hairpin RNA; GFP, green fluorescent protein; E3, ubiquitin-protein isopeptide ligase; APC, adenomatous polyposis coli; DAPI, 4',6'-diamino-2-phenylindole; CAM, chorioallantoic membrane.

generate pCR3.1-Snail-Flag; a bicistronic pCMS-EGFP, to generate pCMS-EGFP-Snail-Flag; and the retroviral vector pBabePuro (5). A human Snail cDNA with both a His<sub>6</sub> and Flag C-terminal epitope tag was cloned into the vector pET21 to generate pET21-Snail-His for expression of recombinant Snail protein in *Escherichia coli*. Snail mutant proteins with Flag epitope tails, including the S100A, S104A, S107A, S100A,S104A, S104A,S107A, S100A,S107A, and S96A mutants, were constructed by PCR-based methods using a wild-type Snail cDNA as a template, followed by subcloning into the pCR3.1 vector. His<sub>6</sub>/Flag-tagged Snail mutants (*i.e.* S104A,S107A and  $\Delta$ 81–109) were also generated by PCR-based methods for expression in bacteria using the pET21 construct. The E-cadherin reporter gene constructs Ecad(–108)-Luc and Ecad(–108)/EboxA.MUT/EboxB.MUT/EboxC.MUT-Luc were described previously (5). A  $\beta$ -TrCP cDNA was obtained by reverse transcription-PCR-based methods, using the total mRNA of 293 cells and the  $\beta$ -TrCP cDNA subcloned into pCR3.1. The dominant negative mouse  $\beta$ -TrCP vector (dn- $\beta$ -TrCP-myc) was kindly provided by Dr. Z. J. Chen (University of Texas-Southwestern, Dallas) (44). A pCR3.1 expression vector encoding HA-tagged ubiquitin was generated by reverse transcription-PCR-based methods using HeLa total RNA. HA-tagged Wnt-1 retroviral expression vector (pLNCX-mWnt-1-HA) was a gift from O. MacDougald (University of Michigan).

To generate the pSUPER-Snail-shRNA, annealed oligonucleotides 5'-GATCCAGGCCTTCAACTGCAAATAGTGTGCTGTCTATTGCA-GTTGAAGCCTTTTTTGGAA-3' and 5'-AGCTTTTCCAAAAAAGG-GCCTTCAACTGCAAATAGGACAGACACACTATTGTCAGTTGAAGG-CCTG-3' were inserted into pSUPER-retro vector (OligoEngine). The 19-nt human Snail target sequence (indicated by underline) was designed and verified to be specific for Snail by Blast search against the human genome and reverse transcription-PCR, respectively. A control shRNA oligonucleotide was used to generate pSUPER-control.

**Cell Culture and Retroviral Gene Expression**—The MCF-7 and 293 cell lines were cultured in Dulbecco's modified Eagle's medium supplemented with 1 mM sodium pyruvate, 100 units/ml penicillin, 100  $\mu$ g/ml streptomycin, and 10% calf serum. pBabePuro-Snail-Flag or pLNCX-mWnt-1-HA were used to generate retroviral stocks in 293 cells for subsequent infection of MCF-7 cells. The stable transfectants MCF-7-Snail-Flag and MCF-7-Wnt-1-HA were obtained from pooled clones selected with 1.0  $\mu$ g/ml puromycin or 400  $\mu$ g/ml geneticin (Invitrogen).

**Recombinant His<sub>6</sub> Fusion Protein and *in Vitro* Phosphorylation**—Recombinant His and Flag double-tagged Snail protein was expressed in pET21-transformed BL21 *E. coli* and purified by nickel-charged agarose affinity chromatography and imidazole elution, according to the manufacturer's protocol (Invitrogen). Two  $\mu$ g of protein was used for *in vitro* phosphorylation with 500  $\mu$ Ci/ $\mu$ mol [ $\gamma$ -<sup>32</sup>P]ATP (ICN), and 75 units of recombinant GSK3 (New England Biolabs, Inc., Beverly, MA) for 2 h at 25 °C.

**Antibodies, Immunoprecipitation, and Immunoblot Analysis**—Snail-Flag proteins were detected by anti-FLAG-M2 antibody (Sigma). Snail-His/Flag proteins were detected with either anti-His<sub>6</sub> or anti-FLAG antibody (BD Biosciences Clontech, Palo Alto, CA), and phosphorylated Snail proteins were detected with anti-phosphoserine antibody (Upstate USA, Inc., Charlottesville, VA).  $\beta$ -TRCP (SC-15354) and GSK3 (4G-1E) antibodies were obtained from Santa Cruz Biotechnology, Inc. (Santa Cruz, CA) and Upstate USA, Inc., respectively. For immunoprecipitation, whole cell Triton X-100 lysates were incubated with FLAG-M2 agarose (Sigma) and washed with lysis buffer. The proteins were resolved by 10% SDS-PAGE and transferred to nitrocellulose, and bound antibodies were visualized with horseradish peroxidase-conjugated secondary antibodies and the ECL system (Pierce) (41). For detecting endogenous Snail,  $\beta$ -catenin, and E-cadherin, nuclear and cytoplasmic fractions (prepared according to the manufacturer's protocol; NucBuster Protein Extraction Kit, Novagen) were prepared from MCF-7 cells. Following SDS-PAGE, proteins were detected with either an anti-Snail polyclonal (5), anti- $\beta$ -catenin (BD Bioscience), anti-E-cadherin (Zymed Laboratories Inc.), or anti- $\beta$ -actin (BD Bioscience) antiserum.

**Pulse-Chase Analysis**—MCF-7 cells or 293 cells were transiently transfected with 1.0  $\mu$ g of pCR3.1-Snail-Flag (FuGENE 6; Roche Applied Science). After 12 h, the medium was changed, and the cells were incubated in standard medium for an additional 48 h, at which point, the cells were pulse-labeled with 50  $\mu$ Ci/ml of [<sup>35</sup>S]Met/Cys (PerkinElmer Life Sciences) for 20 min, washed, and incubated in complete medium for the indicated times. The cell lysates were immunoprecipitated with anti-FLAG-M2-agarose beads, and the samples were subjected to SDS-PAGE and autoradiography.

**siRNA and shRNA Targeting**—293 cells were electroporated with 100 nM siRNA duplexes directed against human GSK3 $\beta$  or a scrambled

mock siRNA (Upstate) 24 h after being transfected with 1.0  $\mu$ g of pCMS-EGFP-Snail-Flag. The cells were harvested 48 h later, and GSK3 and Snail protein levels were determined by immunoblotting with anti-GSK3 and anti-FLAG-M2 antibodies. MCF-7-Wnt-1 cells were transiently co-transfected with 1  $\mu$ g of pSUPER-Snail-shRNA or pSUPER-control, and 0.5  $\mu$ g of a pCMS-EGFP plasmid (BD Biosciences Clontech). The cells were collected 24 h after transfection.

***In Vitro* Translation and *In Vitro* Binding Assay**—[<sup>35</sup>S] $\beta$ -TrCP protein was obtained by *in vitro* transcription and translation from the pCR3.1- $\beta$ -TrCP vector, using the TNT *in vitro* translation system (Promega, Madison, WI) with 10  $\mu$ Ci of [<sup>35</sup>S]Met/Cys (Amersham Biosciences), according to the manufacturer's instruction. Lysates from 293 cells transiently transfected with wild-type or mutant Snail were immunoprecipitated with FLAG-agarose beads, and equivalent amounts of the Snail proteins (normalized by semi-quantitative immunoblot analysis) were incubated with *in vitro* translated [<sup>35</sup>S] $\beta$ -TrCP for an additional 2 h at 25 °C. Specifically bound proteins were eluted, resolved by SDS-PAGE, and visualized by immunoblotting.

***In Vivo* Ubiquitination**—HA-tagged ubiquitin was co-transfected with each FLAG-tagged Snail construct. After 48 h, the lysates were immunoprecipitated and immunoblotted with  $\alpha$ -Flag or anti-HA antibodies.

**Wnt Treatment**—The cell and extracellular protein extracts from Wnt-1 expressing RAC-311 and control MV7 cells (both cell lines kindly provided by L. R. Howe) were prepared from a 0.4 M NaCl buffer extract as described previously (45) and added to cells at a final concentration of 30  $\mu$ g/ml.

**Reporter Gene Assays**—MCF-7 cells were co-transfected with 1.0  $\mu$ g of reporter gene Ecad(–108)-Luc or Ecad(–108)/EboxA.MUT/EboxB.MUT/EboxC.MUT-Luc, 25 ng of wild-type, or mutant Snail expression vectors; MCF-7-Snail-Flag or MCF-7-Wnt-1-HA cells were transfected with 1.0  $\mu$ g of reporter gene only (5). Reporter gene activities were measured with a luciferase assay system (Promega) 48 h after transfection and normalized by measuring  $\beta$ -galactosidase activities of co-transfected pSV-gal (0.25  $\mu$ g; Clontech) with a  $\beta$ -galactosidase enzyme assay system (Promega). Reporter gene activities were presented as relative light units to that obtained from mock transfected cells. The results are expressed as the averages of the ratio of the reporter activities.

**Chick Chorioallantoic Membrane (CAM) Invasion Assay**—Control transfected MCF-7 cells, wild-type Snail-transfected cells, or mutant Snail-transfected cells labeled with fluoresbrite carboxylate microspheres (Polysciences) were cultured atop the CAM of 11-day-old chick embryos for 3 days (25). For analyses of MCF-7-Wnt-1-expressing cells, invasion of the GFP/siRNA co-transfected cells was monitored by GFP fluorescence in place of the fluorescent beads.

**Immunofluorescence**—MCF-7 cells were fixed with 4% formaldehyde, permeabilized with 1% Triton-100, and immunostained with anti-E-cadherin antibody and Alexa-Fluoro-488-labeled anti-mouse secondary antibody (Molecular Probe, Eugene, OR). FLAG-tagged Snail was stained with anti-FLAG polyclonal antibody (Sigma; 1:500) and Alexa-Fluoro-594 labeled anti-rabbit secondary antibody (Molecular Probe). CAM type IV collagen was identified with a chick-specific monoclonal antibody (IIB12) provided by J. Fitch and T. Linsenmayer (Tufts University).

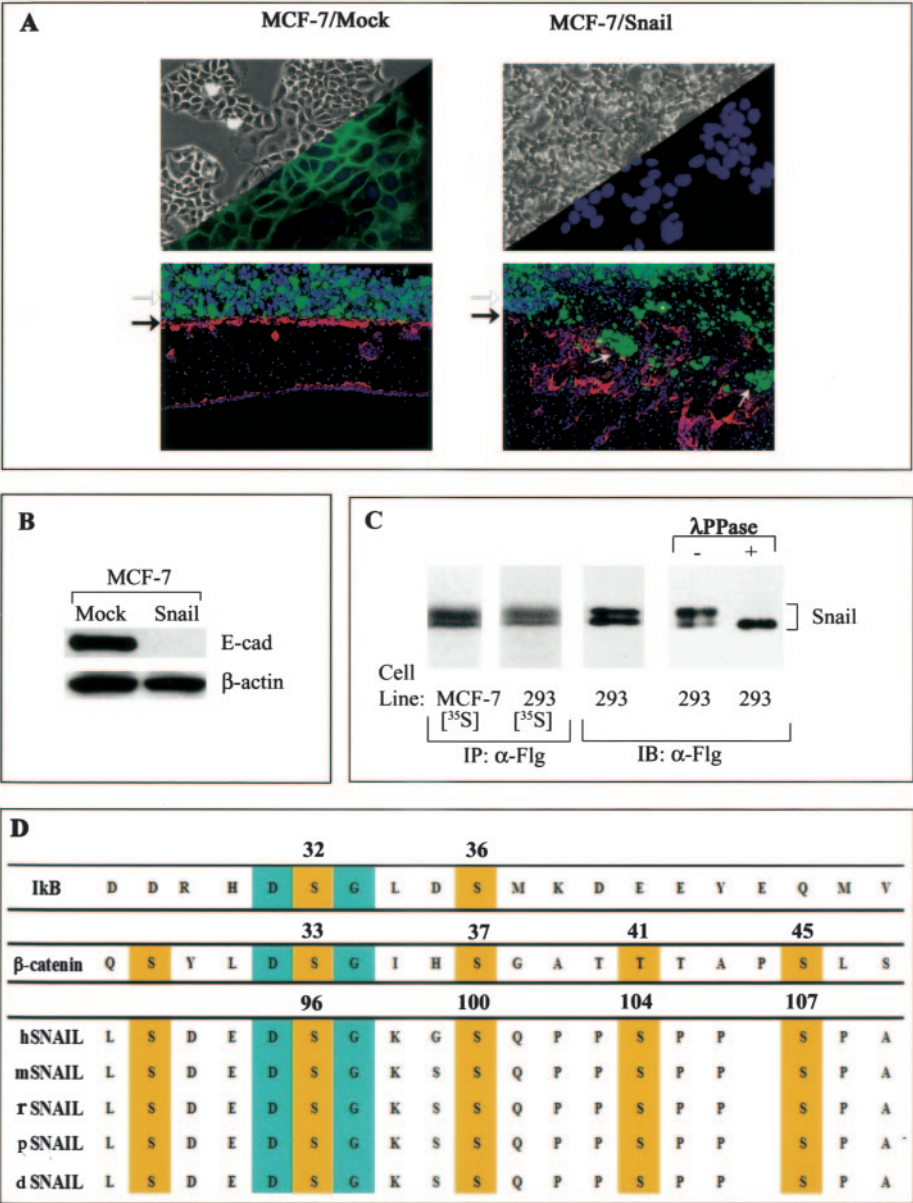
## RESULTS

Following retroviral transduction of MCF-7 cells with a vector encoding a FLAG epitope-tagged form of human Snail (Snail-Flag), the cells displayed a morphology consistent with that seen in a typical EMT, and E-cadherin protein expression was strongly suppressed (Fig. 1, A and B). To determine whether Snail can trigger tissue invasive activity in a manner consistent with the acquisition of a mesenchymal cell-like phenotype, fluorescently labeled MCF-7 cells were cultured atop the chick chorioallantoic membrane. Whereas mock transduced MCF-7 cells were confined to the upper surface of the CAM, the Snail-expressing MCF-7 cells perforated the underlying basement membrane and invaded into the CAM interstitium (Fig. 1A). Interestingly, when the Snail protein was recovered from transfected MCF-7 (or 293) cells, it migrated as a closely spaced doublet, suggesting post-translational modifications (Fig. 1C). Although treatment with O- or N-glycanase failed to alter the migration pattern of Snail (data not shown), treatment of protein extracts with  $\lambda$  protein phosphatase resulted in the loss of the more slowly migrating Snail isoform (Fig. 1C), consistent with notion that Snail is phosphorylated in MCF-7 as well as 293 cells (Fig. 1C). The



FIG. 1. The E-cadherin repressor Snail induces EMT in MCF-7 cells and is a target for phosphorylation.

A, MCF-7 cells, transduced with control (control, empty vector) or Snail-expressing retroviruses, were fixed and stained with an anti-E-cadherin antibody. Phase contrast (upper panels) and indirect immunofluorescence (lower panels) images are displayed (green, E-cadherin; blue, DAPI-stained nuclei). In the lower panels, control or Snail-expressing MCF-7 cells were labeled with fluorescent beads (green) and cultured atop the chick CAM for 3 d. CAMS were fixed, nuclei stained with DAPI (blue), and the CAM basement membrane was stained with anti-chick type IV collagen antibody (red). The frozen sections were examined by fluorescence microscopy. The upper edge of the CAM surface and the tumor mass are marked by black arrows, and open arrows, respectively, while the invasive tumor cells are marked by white arrows. B, E-cadherin protein level in total cell lysates from empty or Snail-transfected MCF-7 cells was assessed by immunoblot analysis with β-actin serving as the loading control. C, MCF-7 or 293 cells were transiently transfected with Snail-Flg and metabolically labeled with [<sup>35</sup>S]Met/Cys. Snail was immunoprecipitated (IP) from cell lysates with α-Flg-agarose beads and subjected to SDS-PAGE followed by autoradiography (lanes labeled [<sup>35</sup>S]) or immunoblot analysis (IB). Following treatment of cell lysates recovered from Snail-Flg-transfected 293 cells with 200 units of λ protein phosphatase (30 min at 37 °C), the Snail doublet detected by α-Flg collapsed to a single, faster migrating band. D, sequence alignment of IκB and β-catenin with human (h), mouse (m), rat (r), pig (p), and dog (d) Snail. Highlights are shown for conserved serine residues (yellow) and the DSG motif (blue).



human Snail amino acid sequence contains in excess of 20 serine and/or threonine residues, but the search for Snail domains that might be phosphorylated was considerably narrowed given that preliminary studies indicated that a mutant form of Snail lacking amino acids 92–120 migrated as a single band (data not shown). Of note, inspection of this region of the Snail protein revealed a <sup>92</sup>SX<sub>2</sub>DSGX<sub>2</sub>SX<sub>3</sub>SX<sub>2</sub>S<sup>107</sup> motif with considerable similarity to the GSK3β-sensitive N-terminal phosphorylation motif found in β-catenin (Fig. 1D) (1, 2). Further, this region of the Snail protein also contained the DSGXXS destruction motif recognized by β-TrCP in β-catenin as well as the IκB protein (Fig. 1D) (1, 2). Consistent with the possibility that Snail, like β-catenin, is recognized and bound by GSK3β (1, 2), immunoprecipitates of Snail-Flg recovered from transfected 293 cells contained endogenous GSK3β (Fig. 2A). In light of the existence of multiple potential phosphorylation sites within the amino acid 92–120 region of Snail, a series of single, or double, Ser → Ala substitutions were generated in the Snail-Flg expression vector. The constructs encoding the Snail mutants were then expressed in 293 cells, and the electrophoretic mobility of the Snail-Flg proteins was examined prior to and following λ protein phosphatase treatment of the cell extracts. Although single Ser → Ala substi-

tutions at Ser<sup>100</sup> (S100A), Ser<sup>104</sup> (S104A), or Ser<sup>107</sup> (S107A) or double substitutions at Ser<sup>100</sup>/Ser<sup>104</sup> (S100A,S104A) or Ser<sup>100</sup>/Ser<sup>107</sup> (S100A,S107A) did not affect the λ protein phosphatase-induced gel shift, dual Ser → Ala mutations at Ser<sup>104</sup> and Ser<sup>107</sup> (S104A,S107A) ablated the gel shift associated with λ protein phosphatase treatment (Fig. 2B). A key role for the Ser<sup>104</sup> and Ser<sup>107</sup> residues was further corroborated by data showing that recombinant GSK3β directly phosphorylated wild-type Snail via a LiCl-sensitive process *in vitro* (17) but not the S104A,S107A double mutant form of Snail (Fig. 2C). Indeed, whereas pulse-chase analysis demonstrated wild-type Snail was rapidly degraded in the course of a 4-h chase period, expression levels of the S104A,S107A mutant remained stable (Fig. 2D). The inability of GSK3β to phosphorylate the S104A,S107A mutant Snail protein *in vivo* could conceivably reflect nonspecific alterations in the conformation of the mutant Snail (18). However, consistent with the notion that Snail is phosphorylated *in vivo* by GSK3β, phosphorylation of wild-type Snail in 293 cells was blocked by treatment of the cells with the GSK3β inhibitor, LiCl (Fig. 2E) (17, 18). Coincident with the LiCl-dependent inhibition of Snail phosphorylation, steady state levels

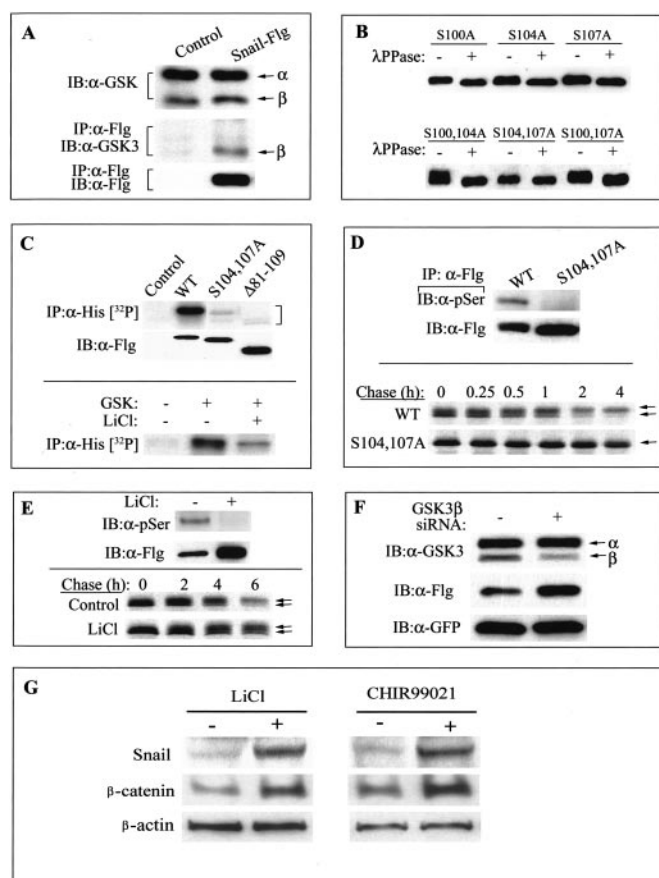


**FIG. 2. GSK3 $\beta$ -dependent Snail phosphorylation.** A, GSK3 (both  $\alpha$  and  $\beta$ ) were detected in control and Snail-Flg-transfected 293 cell lysates by immunoblot analysis (*top panel*). GSK3 $\beta$ -Snail complexes were isolated in immunoprecipitates recovered from lysates of control or Snail-Flg-transfected 293 cells following pull-down with  $\alpha$ -Flg-agarose beads, SDS-PAGE, and immunoblot with anti-GSK3 antibody (*middle panel*). Snail protein levels in the control or Snail-Flg-transfected cells were assessed by  $\alpha$ -Flg blot (*bottom panel*). B, Flg-tagged Snail mutants harboring Ser  $\rightarrow$  Ala substitutions were expressed in 293 cells, lysates from the transfectants incubated with or without  $\lambda$  protein phosphatase, and changes in Snail mobility analyzed by  $\alpha$ -Flg immunoblot. C, His-tagged recombinant wild-type Snail, S104A, S107A mutant Snail, or a  $\Delta$ 81–109 Snail deletion mutant (2  $\mu$ g of protein each) were incubated with recombinant GSK3 $\beta$  and [ $\gamma$ - $^{32}$ P]ATP for 2 h at 25  $^{\circ}$ C. Phosphorylated and total Snail protein were resolved by SDS-PAGE and visualized by autoradiography or  $\alpha$ -Flg blot (*top panel*). Snail phosphorylation by GSK3 $\beta$  was inhibited by LiCl (20 mM) (*bottom panel*). D, wild-type or S104A, S107A mutant Snail-Flg was expressed in 293 cells, immunoprecipitated (IP) with  $\alpha$ -Flg, and immunoblotted (IB) with either anti-phosphoserine (*anti-pSer*) or  $\alpha$ -Flg antibodies (*top panel*). Following a 20-min pulse with [ $^{35}$ S]Met/Cys, 293 cells transfected with wild-type Snail-Flg or S104A, S107A Snail-Flg were lysed at the indicated times, and  $\alpha$ -Flg immunoprecipitates were resolved by SDS-PAGE and visualized by autoradiography (*bottom panel*). E, phosphorylated and total Snail protein levels were monitored in Snail-Flg-transfected 293 cells incubated with or without 40 mM LiCl for 18 h (*top panel*). Snail half-lives in LiCl-treated cells were measured by pulse-chase analysis (*bottom panel*) as described above. F, 293 cells were transiently transfected with a GFP-Snail-Flg expression vector and either GSK3 $\beta$  or scrambled siRNA duplexes. GSK3- $\alpha/\beta$  and Snail levels were monitored by anti-GSK3 and  $\alpha$ -Flg immunoblot. GFP, detected with  $\alpha$ -GFP, was used as the loading control. G, MCF-7 cells ( $1 \times 10^6$ ) were incubated in the absence or presence of LiCl (40 mM) or CHIR99021 (2  $\mu$ M) for 8 h. Following SDS-PAGE of nuclear extracts, endogenous Snail and  $\beta$ -catenin and actin were detected by immunoblot. Nuclear  $\beta$ -actin was used as a loading control.

of wild-type Snail were also increased in LiCl-treated cells (Fig. 2E). Additionally, pulse-chase data indicated that LiCl treatment prolongs the half-life of the faster migrating and presumably hypophosphorylated or nonphosphorylated form(s) of Snail (Fig. 2E). Using a siRNA knockdown approach to reduce

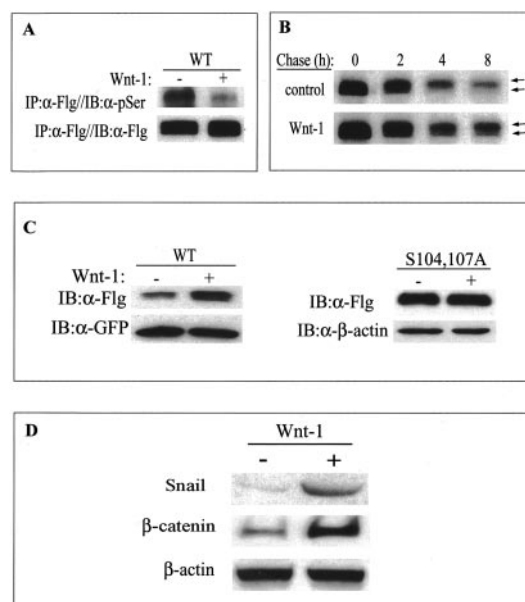


**FIG. 3. Wnt-1 regulation of Snail phosphorylation.** A, 293 cells transfected with Snail-Flg were treated with control or Wnt-1-conditioned medium for 18 h. Phosphorylated Snail levels were determined following immunoprecipitation (IP,  $1\times$  and  $0.5\times$  volume of the respective cell lysates) with  $\alpha$ -Flg and immunoblotting (IB) with anti-Ser(P) (*anti-pSer*). B, Snail half-life in control or Wnt-1-treated 293 cells was determined by pulse-chase analysis and SDS-PAGE/autoradiography of  $\alpha$ -Flg immunoprecipitates. C, 293 cells were transfected with either GFP-Snail-Flg or S104A, S107A Snail-Flg and incubated with control or Wnt-1-conditioned cell extracts for 18 h. Snail, GFP, and  $\beta$ -actin were detected by  $\alpha$ -Flg,  $\alpha$ -GFP, and  $\alpha$ - $\beta$ -actin immunoblot. D, MCF-7 cells ( $1 \times 10^6$ ) were incubated with control or Wnt-1-conditioned cell extracts for 18 h. MCF-7 nuclear extracts were immunoblotted for endogenous snail or  $\beta$ -catenin with nuclear  $\beta$ -actin serving as a loading control. WT, wild type.

endogenous GSK3 $\beta$  levels in 293 cells engineered to ectopically express Snail, the steady state levels of Snail protein were likewise increased (Fig. 2F). To further determine whether GSK3 $\beta$  regulates the endogenous level of Snail in a fashion similar to that observed for the exogenously expressed protein, MCF-7 cells were cultured in the presence of either LiCl or the GSK3-specific inhibitor, CHIR99021 (19). As expected, GSK3 inhibition by either reagent induced significant increases in the steady state nuclear levels of endogenous Snail in tandem with similar increases in  $\beta$ -catenin (Fig. 2G).

*In vivo*, a subset of Wnt family members trigger largely undefined pathways that lead to the inhibition of GSK3 $\beta$  activity (1, 20). Because Wnt expression occurs frequently in a temporal fashion coincident with developmental EMT programs (1, 20–22), we sought to determine whether GSK3 $\beta$ -dependent phosphorylation of Snail could be inhibited by Wnt-1. Indeed, the phosphorylation of ectopically expressed wild-type Snail was suppressed markedly by treatment of the cells with Wnt-1-conditioned medium, and in concert, Snail half-life was increased (Fig. 3, A and B). Although Wnt-1 also increased the steady state expression levels of wild-type Snail, no effect was observed on the levels of the S104A, S107A mutant (Fig. 3C). Consistent with the premise that GSK3 $\beta$  regulates Snail and  $\beta$ -catenin levels in a cooperative fashion, Wnt-1 signaling mediated tandem increases in the nuclear levels of endogenous Snail as well as  $\beta$ -catenin (Fig. 3D).

Following the GSK3 $\beta$ -dependent phosphorylation of  $\beta$ -catenin, a  $^{32}$ DpSGXXpS motif in the post-translationally modified protein is recognized by the E3 ubiquitin ligases  $\beta$ -TrCP1 or  $\beta$ -TrCP2, which mediate the ubiquitination of phosphorylated  $\beta$ -catenin and target the protein for subsequent degradation in

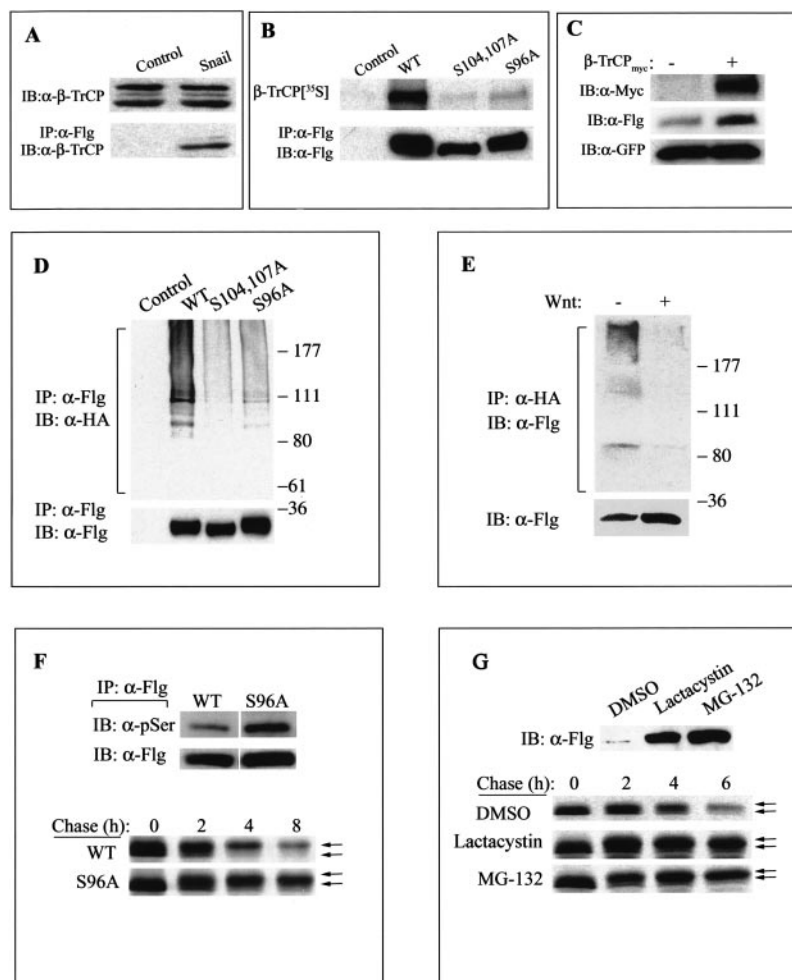


**FIG. 4. Phosphorylation-dependent Snail ubiquitination and proteasomal degradation.** *A*, endogenous  $\beta$ -TrCP isoforms were detected in lysates of control or Snail-Flag-transfected 293 cells (upper panel).  $\beta$ -TrCP1-Snail-Flag complexes were identified in  $\alpha$ -Flag-agarose immunoprecipitates following immunoblotting (IB) with anti- $\beta$ -TrCP (lower panel). *B*, equivalent amounts of wild-type Snail, S107,104A, and Ser<sup>96</sup>  $\rightarrow$  Ala Snail proteins were harvested from transfected 293 cells, immobilized on  $\alpha$ -Flag-agarose beads, and incubated with *in vitro* translated [<sup>35</sup>S] $\beta$ -TrCP1; bead-bound protein was resolved by SDS-PAGE and autoradiography (upper panel) or detected by  $\alpha$ -Flag immunoblotting (lower panel). *C*, 293 cells were transfected with a pCMS-EGFP-Snail-Flag alone or with dN-TrCP1-Myc for 48 h. Protein levels of dN-TrCP1 were detected with anti-Myc (top panel), Snail with anti-FLAG (middle panel), and anti-GFP as control (bottom panel) by Western blot. *D*, 293 cells were co-transfected with HA-tagged ubiquitin and wild-type (WT), S104A, S107A, or S96A Snail. Following immunoprecipitation (IP) with  $\alpha$ -Flag, ubiquitinated Snail (upper panel) was visualized following SDS-PAGE and anti-HA ( $\alpha$ -HA) immunoblotting. Snail monomers were detected by immunoprecipitating and immunoblotting with  $\alpha$ -Flag (lower panel). *E*, 293 cells expressing Snail-Flag and HA-tagged ubiquitin were incubated with control or Wnt-1-conditioned cell extracts for 18 h. Snail monomers and high molecular weight forms of Snail were detected by immunoprecipitation ( $\alpha$ -HA) and immunoblotting with  $\alpha$ -Flag. *F*, the phosphorylation (upper panel) and half-life (lower panel) of wild-type versus S96A Snail protein were monitored in 293 cells transfected with the respective FLAG-tagged Snail constructs. *G*, 293 cells transfected with a wild-type Snail-Flag expression vector were incubated with lactacystin (5  $\mu$ M), MG-132 (5  $\mu$ M), or Me<sub>2</sub>SO (DMSO) for 18 h. Lysates from Me<sub>2</sub>SO- or inhibitor-treated cells (1.0 and 0.2  $\mu$ g of total protein, respectively) were immunoblotted for Snail protein content (upper panel). Pulse-chase analysis of Snail-Flag half-life was likewise performed in proteasome inhibitor-treated cells (lower panel). Inhibitors were added to the transfected cells 1 h before the pulse and included during the entire chase period.

the proteasome (1, 2, 23). To determine whether  $\beta$ -TrCP recognized the homologous <sup>95</sup>DSGXXS motif found in Snail, a FLAG epitope-tagged wild-type Snail protein was ectopically expressed in 293 cells. Following immunoprecipitation of the extracts with an anti-FLAG antibody, endogenous  $\beta$ -TrCP1 protein was found to be specifically recovered in association with Snail (Fig. 4A). Furthermore, [<sup>35</sup>S]Met-labeled  $\beta$ -TrCP1 prepared by *in vitro* translation was shown to bind to the wild-type Snail protein recovered from lysates of transfected 293 cells (Fig. 4B). However,  $\beta$ -TrCP1 was unable to form a stable complex with either the phosphorylation-resistant S104A, S107A mutant Snail protein or the Snail mutant harboring a single Ser<sup>96</sup>  $\rightarrow$  Ala substitution within the putative  $\beta$ -TrCP1-binding domain (Fig. 4B). Consistent with these findings, the steady state levels of wild-type Snail were enhanced by co-expressing a dominant negative form  $\beta$ -TrCP1 in 293

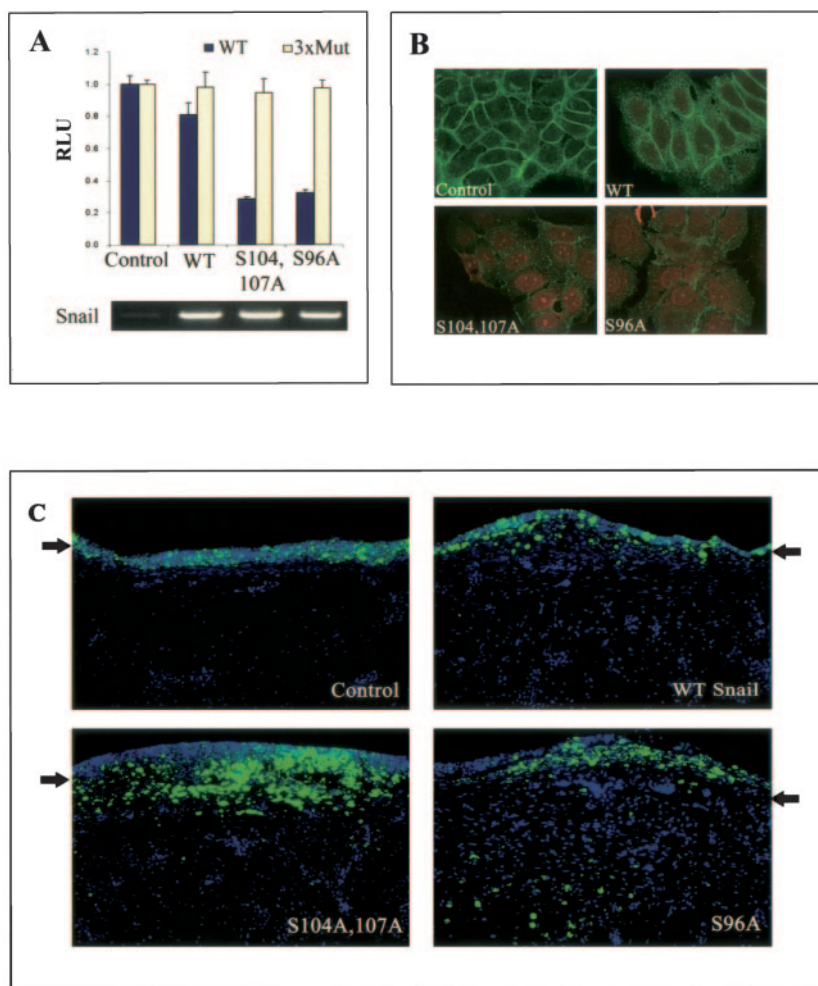
cells (Fig. 4C) as well as MCF-7 cells (data not shown).

In a fashion similar to that described for  $\beta$ -catenin (1, 2, 22), further studies demonstrated that wild-type Snail protein undergoes rapid ubiquitination *in vivo* (Fig. 4D). By contrast, ubiquitination of Snail proteins containing mutations at either key phosphorylation or recognition sites (*i.e.* Ser<sup>104</sup>/Ser<sup>107</sup> or Ser<sup>96</sup> within the DSG destruction motif) was strongly suppressed, as was the formation of high molecular weight Snail complexes in Wnt-1-treated cells (Fig. 4, D and E). Although the Ser<sup>96</sup>  $\rightarrow$  Ala mutant Snail protein was phosphorylated in 293 cells, the loss of this key phosphorylation site within the DSG destruction motif resulted in the failure of the protein to be recognized and ubiquitinated by  $\beta$ -TrCP, resulting in an increased steady state level and prolonged half-life of the mutant (Fig. 4, B, D, and F). Indeed, the half-life of the Ser<sup>96</sup>  $\rightarrow$  Ala mutant Snail protein was similar to that observed follow-



**FIG. 5. Regulation of E-cadherin repressor and invasive activities by degradation-resistant Snail mutants.**

**A**, the E-cadherin repressor activity of wild-type, S104A, S107A, and S96A Snail were assessed with the reporter construct, Ecad(-108)-Luc, which contains the wild-type (WT) promoter sequence from nt -108 to +125 of the endogenous E-cadherin promoter or a control construct, Ecad(-108)/EboxA.MUT/EboxB.MUT/EboxC.MUT-Luc, which harbors mutations in all three E-boxes (3 $\times$ Mut). Snail mRNA levels in each of the transfectants was monitored by reverse transcription-PCR. **B**, E-cadherin expression in MCF-7 cells transiently transfected with wild-type S104A, S107A or S96A Snail was assessed by indirect immunofluorescence with anti-E-cadherin mAb (green). Snail was stained with  $\alpha$ -Flg rabbit polyclonal antibody (red). The images were obtained by confocal microscopy. **C**, MCF-7 cells were transiently transfected with control, wild-type, S104-107A, or S96A Snail, labeled with fluorescent beads (green) and cultured atop the chick CAM for 3 days. CAMs were fixed, cell nuclei were stained with DAPI (blue), and tissue sections were examined by fluorescence microscopy. The upper edge of the CAM surfaces is marked by the black arrows. The numbers of invaded cells were counted in 10 randomly selected fields for each experiment and expressed as the means  $\pm$  S.D. (control,  $0 \pm 0$ ; wild type,  $4 \pm 2$ ; S104A, S107A,  $30 \pm 6$ ; and S96A,  $48 \pm 4$ ).



ing treatment of 293 cells expressing wild-type Snail protein with the proteasome inhibitors lactacystin or MG-132 (Fig. 4G).

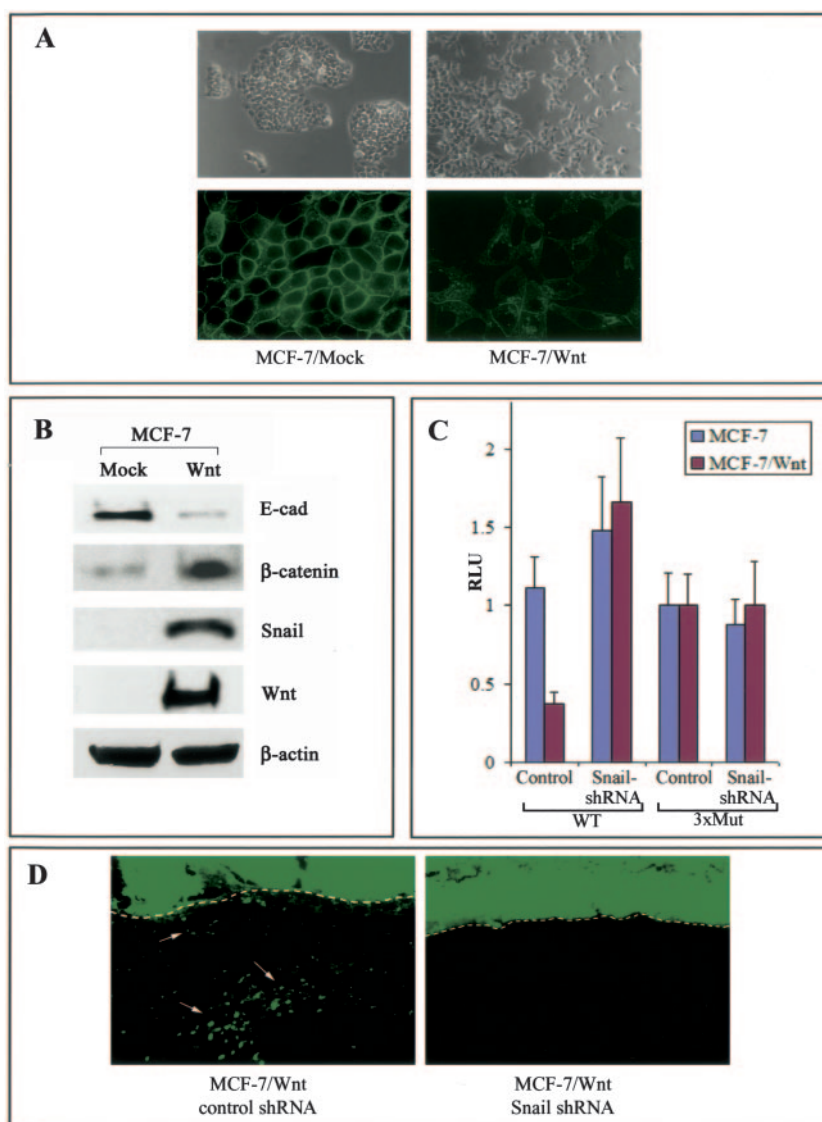
Snail has been proposed to play a key role during both development and cancer by virtue of its ability to repress E-cadherin expression and drive EMT (3–5). To assess the consequences of Snail stabilization on its E-cadherin repressor activity, we compared the relative abilities of wild-type Snail and the S104A, S107A or Ser<sup>96</sup>  $\rightarrow$  Ala mutants to regulate an E-cadherin promoter gene construct previously shown to be Snail-sensitive (3–5). Because Snail has been implicated in repression of E-cadherin transcription through the three E-box domains present in the proximal E-cadherin promoter region, a control version of the construct was employed wherein all three E-box domains were mutated (3 $\times$ Mut) (5). Whereas limiting amounts (25 ng) of the expression vector encoding wild-type Snail exerted only modest inhibitory effects on the wild-type E-cadherin reporter gene construct in MCF-7 cells, equivalent amounts of the expression vectors encoding the Ser<sup>104</sup>/Ser<sup>107</sup> or Ser<sup>96</sup>  $\rightarrow$  Ala mutants exerted stronger repression effects on E-cadherin promoter activity (Fig. 5A). An analysis of the levels of Snail transcripts expressed ectopically in the cells confirmed that the differences in repressor activity observed between the wild-type and mutant Snail constructs did not result from variations in the mass of DNA transfected or the levels of transcripts produced from the vectors (Fig. 5A). When compared with wild-type Snail, the Ser<sup>104</sup>/Ser<sup>107</sup> and Ser<sup>96</sup>  $\rightarrow$  Ala mutants also displayed an enhanced activity to suppress endogenous E-cadherin expression in transfected MCF-7 cells (Fig. 5B). Although phosphorylation of Snail has been reported to regulate its nuclear localization and repressor activity by

modulating the activity of a nuclear export sequence located between residues 132 and 143 (24), both the Ser<sup>104</sup>/Ser<sup>107</sup> and Ser<sup>96</sup>  $\rightarrow$  Ala mutants were preferentially localized to the nuclear compartment in a fashion comparable with wild-type Snail following transfection into MCF-7 cells (Fig. 5B).

To address the possibility that stabilized Snail might play an exaggerated role in engaging an EMT program capable of promoting an invasive phenotype, MCF-7 cells were transiently transfected with wild-type Snail or either of the S104A, S107A or Ser<sup>96</sup>  $\rightarrow$  Ala mutants, and the *in vivo* invasive behavior of the MCF-7 transfectants was assessed by culturing the cells atop the chick CAM. Although control transfected MCF-7 cells were unable to penetrate the CAM surface, both the S104A, S107A and the Ser<sup>96</sup>  $\rightarrow$  Ala mutants induced a more aggressive tissue invasive program than wild-type Snail (Fig. 5C).

Finally, given the ability of Wnt-1 to induce the up-regulation of endogenous levels of nuclear Snail protein, coupled with its ability to repress E-cadherin expression and support a tissue invasive EMT program, we sought to determine whether Wnt-1 drives EMT via a Snail-dependent process. Indeed, following Wnt-1-transduction, MCF-7 cells adopted a fibroblastic phenotype, down-regulated E-cadherin levels, increased nuclear concentrations of  $\beta$ -catenin and Snail proteins, and suppressed E-cadherin promoter activity (Fig. 6, A–C). Moreover, consistent with the proposition that a Wnt-driven EMT program has been induced, the Wnt-1-transduced MCF-7 cells expressed tissue invasive activity similar to that observed with Snail-transduced cells (compare Fig. 6C with Fig. 1A). If, however, Snail expression in Wnt-transduced MCF-7 cells was targeted with any one of four different shRNA constructs, Snail

**FIG. 6. Involvement of Snail in Wnt-induced down-regulation of E-cadherin and invasion.** A, MCF-7 cells, transduced with control (control, empty vector) or WNT-1-expressing retroviruses, or fixed and stained with anti-E-cadherin antibody. Phase contrast (*upper panels*) and indirect immunofluorescence (*lower panels*) images are displayed (*green*, E-cadherin). B, endogenous E-cadherin,  $\beta$ -catenin and Snail protein levels were detected in cytoplasmic (E-cad) or nuclear ( $\beta$ -catenin and Snail) fractions of MCF-7-Wnt-1-HA (MCF-7/Wnt) and MCF-7-mock cells with immunoblotting. Wnt expression was confirmed by anti-HA blot with nuclear  $\beta$ -actin levels monitored as the loading control. C, the E-cadherin promoter activities in MCF-7/Wnt, MCF-7-Snail-Flg, and mock transfected cells were examined by reporter gene assays with Ecad(-108)-Luc or Ecad(-108)/EboxA.MUT/EboxB.MUT/EboxC.MUT-Luc (3 $\times$ Mut) following co-transfection with Snail-specific or control shRNA expression vectors, respectively. D, MCF-7/Wnt cells were transiently co-transfected with either a Snail-specific or control shRNA vector and a GFP expression vector. The cells were cultured atop the CAM for 3 days. Fixed tissue sections were examined by fluorescence microscopy for GFP-positive cells. The upper face of the CAM surfaces is indicated by the *dashed white lines*. Similar if not identical inhibition of invasion was obtained with three other anti-Snail shRNA constructs targeted against distinct sequences as well as two distinct sets of anti-Snail siRNA duplexes (data not shown).



mRNA expression was inhibited completely (data not shown), the suppression of E-cadherin promoter activity was reversed (Fig. 6B), and tissue invasive activity was lost (Fig. 6C). By contrast, transfection with a control shRNA neither affected E-cadherin promoter activity or invasion (Fig. 6, B and C). Hence, Snail plays a key role in regulating Wnt-1-induced EMT in MCF-7 cells.

#### DISCUSSION

Snail plays a key role in EMT processes characterizing tumor progression, as well as developmental programs ranging from gastrulation to neural crest formation (6). The unexpected identification of a  $\beta$ -catenin-like consensus motif in the N-terminal domain of Snail that supports its GSK3 $\beta$ -dependent phosphorylation,  $\beta$ -TrCP-dependent ubiquitination, and proteosomal degradation highlights a new model wherein Wnt signaling participates in the co-regulation of Snail-driven as well as  $\beta$ -catenin/LEF-1-driven transcriptional programs. With regard to  $\beta$ -catenin, its dual phosphorylation by GSK3 $\beta$  and casein kinase-1 appears to take place in a multi-protein complex that includes adenomatous polyposis coli (APC) and Axin tumor suppressor proteins (1, 26, 27). Although a required role for casein kinase-1 in generating a phosphoserine priming site in  $\beta$ -catenin for subsequent GSK3 $\beta$ -mediated phosphorylation remains controversial (28), our preliminary studies suggest

that casein kinase-1 can phosphorylate Snail *in vitro*.<sup>2</sup> The ability of GSK3 $\beta$  to phosphorylate primed *versus* unprimed Snail *in vivo*, however, requires further study. These findings notwithstanding, it is conceivable that Snail, like  $\beta$ -catenin, might be stabilized by mutations in APC, Axin, or the Snail transcript itself, thus predisposing to the development of carcinogenic states (3–5, 29). However, because increasing evidence supports important roles for the activation of canonical Wnt signaling in normal as well as neoplastic states (12–15, 30, 31), inappropriate activation of Snail-dependent transcriptional programs are not necessarily constrained to pathological processes that require somatic mutations in the Snail gene itself or accessory molecules that regulate its phosphorylation and degradation.

During embryogenesis, E-cadherin down-regulation appears to be temporally linked to fibroblast growth factor signaling, Snail expression, and activation of the canonical Wnt signaling cascade (9–11, 20, 21, 32). Recent studies suggest that  $\beta$ -catenin, upon its association with the TCF transcription factor family member, LEF-1, can act in a cooperative fashion with Snail to suppress E-cadherin transcription via LEF-1/ $\beta$ -catenin

<sup>2</sup> J. In Yook, X.-Y. Li, E. R. Fearon, and S. J. Weiss, unpublished observation.



TABLE I  
Snail serine-rich region sequence alignment

	92	96	100	104	107	111	115	119
<b>Homo sapiens</b> (NP_005976.2)	L S D E	D S G	- K G S	Q P P S	P P S	P A P S	S S F S	S T S V S
<b>Gallus gallus</b> (NP_990473.1)	S S E E	D E G	- K S S	G P P S	P A S	A P A A	A E R F	R C A Q
<b>Mauremys caspica</b> (AAN62359.1)	S S E E	D E G	- K T S	D P P S	P A S	S A T E	A E K F	Q C S Q
<b>Xenopus laevis</b> (P19382)	F S S E	D E G	G K T S	D P P S	P A S	S A T E	A E K F	Q C N Q
<b>Zebra fish</b> (CAA92795.1)	S G E E	D E G	- R T S	D P P S	P D S	S D T Y	H P Q Q	T S R R

interactions with sequences upstream of the E-cadherin promoter (11). Our findings raise the possibility of a more complex and interdigitated scheme wherein exposure of normal or neoplastic cells to a combination of Snail-inducing growth factors and Wnts would stabilize the intracellular levels of the Snail and  $\beta$ -catenin proteins by as yet undefined mechanisms that serve to shield these regulatory molecules from GSK3 $\beta$ -dependent phosphorylation (1, 20, 33). In turn, Snail acting as a transcriptional repressor of E-cadherin potentially facilitates the intracellular transfer of E-cadherin-bound  $\beta$ -catenin to a Wnt-stabilized "signaling" pool (3–5, 9). Snail might further synergize with the Wnt/ $\beta$ -catenin axis by inducing LEF-1 expression either directly or by suppressing BMP expression (11, 29, 34). Additional studies are needed to determine the relative roles that stabilized Snail and  $\beta$ -catenin (and perhaps,  $\gamma$ -catenin) (35) play in coordinating Wnt-induced EMT programs, but Snail appears to play a dominant, if not required, role in driving the tissue invasive process in MCF-7 breast carcinoma cells. Given the parallels noted between developmental and neoplastic EMT programs (6), these findings are consistent with a required role for Snail during formation of the mesoderm germ layer (36).

Interestingly, our results complement and extend a very recent report by Zhou *et al.* (37) that similarly describes a role for GSK3 $\beta$  in regulating Snail phosphorylation and activity. In a variation of the theme presented here, these investigators proposed that Snail displays two distinct GSK3 $\beta$  consensus motifs. The first GSK3 $\beta$  recognition sequence, as in our study, centers on the putative  $\beta$ -TrCP binding site at Ser(P)<sup>96</sup> and Ser(P)<sup>100</sup>. They then propose that a second motif, <sup>107</sup>SXXX-SXXXSXXXS<sup>119</sup>, regulates the export of nuclear Snail into the cytosolic space as a consequence of an independent series of GSK3 $\beta$ -dependent phosphorylations (37). Further work is required to cohesively mesh this model with our independent findings that describe a dominant role for Ser<sup>104</sup> and Ser<sup>107</sup> in regulating Snail phosphorylation and activity. However, it should be noted that GSK3 $\beta$  effectively phosphorylates serine or threonine residues *in vivo* only when a phosphoserine or phosphothreonine is positioned four amino acids C-terminal to the new phosphorylation site (18). Hence, we tentatively favor a working model wherein a priming event first occurs at Ser<sup>104</sup> that would simultaneously support the serial GSK3 $\beta$ -dependent phosphorylation of Ser<sup>100</sup>, Ser<sup>96</sup>, and possibly Ser<sup>92</sup> as well as the casein kinase-1-dependent phosphorylation of Ser<sup>107</sup> (18). Although mass spectrometric analyses will help resolve these issues, it should be emphasized that our findings further diverge from those of Zhou *et al.* with regard to the functional ramifications of the GSK3 $\beta$ -Snail axis (37, 38). In contrast with our report, these investigators reported that wild-type Snail, even when overexpressed in MCF-7 cells, is unable to induce EMT (37). Further, although Wnt signaling was not examined in their study, no agonists could be identified that were able to either induce increases in endogenous Snail or engage Snail-dependent EMT (37, 38). Instead, EMT was only observed

when a series of six Ser  $\rightarrow$  Ala substitutions were introduced into the Snail protein at Ser<sup>96</sup>, Ser<sup>100</sup>, Ser<sup>107</sup>, Ser<sup>111</sup>, Ser<sup>115</sup>, and Ser<sup>119</sup>, and the mutant construct was overexpressed in target cells (37). Hence, our demonstration that Wnt signaling not only regulates endogenous Snail but also drives Snail-dependent EMT represents the first functional demonstration of the potential importance of this pathway in neoplastic cells.

By embedding within Snail a series of  $\beta$ -catenin-like recognition motifs for GSK3 $\beta$  and  $\beta$ -TrCP, a cooperative system appears to have evolved that allows for the tandem regulation of Snail- and  $\beta$ -catenin-TCF-regulated target genes as they converge on the EMT process. Of note, although the <sup>92</sup>SX<sub>2</sub>DSGX<sub>2</sub>SX<sub>3</sub>SX<sub>2</sub>S<sup>107</sup> motif is conserved in human as well as other mammals (Fig. 1), substitutions are observed in more distantly related vertebrate species (Table I) where it has already been noted that Snail family members display highly divergent N-terminal regions (6). Although differences in Snail function among species make direct comparisons between conserved regions difficult to interpret (*e.g.* Slug, rather than Snail, plays the dominant role in driving EMT in the chick) (6), the Ser<sup>96</sup>  $\rightarrow$  Glu substitution is consistent with more recent studies demonstrating the ability of  $\beta$ -TrCP to both recognize a charged glutamate residue in place of a Ser(P) moiety (39) as well as target substrates harboring a DSX<sub>n</sub>S motif where  $n > 2$  (23). We do note, however, that the bulk of the putative nuclear localization signal assigned by Zhou *et al.* to the <sup>111</sup>SXXXSXXXS<sup>119</sup> motif (37) is not conserved in lower vertebrates (Table I). This caveat aside, it appears that a common but modified scheme for regulating Snail activity may extend beyond mammals to include less closely related vertebrate species where constraints specific to given organisms have resulted in the evolution of a set of similar, yet distinct, molecular solutions.

Until recently, attention has focused on the role of mutational defects in APC,  $\beta$ -catenin, and Axin in activating the Wnt/ $\beta$ -catenin-TCF pathway in human cancer. Intriguingly, although mutational defects in  $\beta$ -catenin, Axin, and APC are fairly common in certain cancer types, in other neoplastic states such as breast cancer, mutational defects in well defined components of the canonical Wnt pathway have only very rarely been identified (5, 40). These findings could be interpreted as evidence that Wnt signaling cascades play only a limited role in the development and progression of breast and other cancers where mutational defects in the canonical Wnt signaling pathway have rarely been seen. However, recent studies have suggested an important functional role for Wnt signals in various cancers and the possibility that nonmutational mechanisms may activate Wnt signaling via either enhanced local (autocrine or paracrine) expression of Wnts, epigenetic inactivation of the expression of Wnt antagonists (such as secreted frizzled-related proteins of Wnt inhibitory factor-1), or the up-regulation of potential GSK3 $\beta$  inhibitory factors (12, 14, 16, 40). Curiously, and inconsistent with the view that Wnt signals in cancer cells transmit their effects solely via stabili-

zation of  $\beta$ -catenin, a requirement for upstream Wnt ligand function/activity has even been implicated in cancers with constitutive deregulation of  $\beta$ -catenin resulting from APC or  $\beta$ -catenin mutations (13–15). Taken together, these data support a model wherein inappropriate activation of the Wnt-GSK3 $\beta$  signaling cascade regulates carcinoma cell phenotype not only via effects on  $\beta$ -catenin-TCF-dependent transcription but also through the ability of the Wnt-GSK3 $\beta$  signaling cascade to activate Snail-driven transcriptional programs. Indeed, given that Snail activity extends beyond the regulation of EMT-related processes to include cell death and growth (8, 41–43), our findings support a new operating platform by which canonical Wnt signals can regulate tumor cell phenotype.

**Acknowledgments**—We thank Philip Cohen (University of Dundee) for helpful discussions and Rudolpho Marquez (University of Dundee) for providing CHIR99021.

## REFERENCES

- Nelson, W. J., and Nusse, R. (2004) *Science* **303**, 1483–1487
- Conacci-Sorrell, M., Zhurinsky, J., and Ben-Ze'ev, A. (2002) *J. Clin. Invest.* **109**, 987–991
- Batlle, E., Sancho, E., Franci, C., Dominguez, D., Monfar, M., Baulida, J., and Garcia De Herreros, A. (2000) *Nat. Cell Biol.* **2**, 84–89
- Cano, A., Perez-Moreno, A. M., Rodrigo, I., Locascio, A., Blanco, M. J., del Barrio, M. G., Portillo, F., and Nieto, M. A. (2000) *Nat. Cell Biol.* **2**, 76–83
- Hajira, K. M., Chen, D. Y. S., and Fearon, E. R. (2002) *Cancer Res.* **62**, 1613–1618
- Nieto, M. A. (2002) *Nat. Rev. Mol. Cell Biol.* **3**, 155–166
- Fujita, N., Jaye, D. L., Kajita, M., Geigerman, C., Moreno, C. S., and Wade, P. A. (2003) *Cell* **113**, 207–219
- Palmer, H. G., Larriba, M. J., Garcia, J. M., Ordonez-Moran, P., Pena, C., Peeiro, S., Puig, I., Rodriguez, R., de la Fuente, R., Bernad, A., Pollan, M., Bonilla, F., Gamallo, C., de Herreros, A. G., and Munoz, A. (2004) *Nat. Med.* **10**, 917–919
- Ciruna, B., and Rossant, J. (2001) *Dev. Cell* **1**, 37–49
- Garcia-Castro, M. I., Marcelle, C., and Bronner-Fraser, M. (2002) *Science* **297**, 848–851
- Jamora, C., DasGupta, R., Koceniowski, P., and Fuchs, E. (2003) *Nature* **422**, 317–322
- Uematsu, K., He, B., You, L., Xu, Z., McCormick, F., and Jablons, D. M. (2003) *Oncogene* **22**, 7218–7221
- He, B., You, L., Uematsu, K., Xu, Z., Lee, A. Y., Matsangou, M., McCormick, F., and Jablons, D. M. (2004) *Neoplasia* **6**, 7–14
- Suzuki, H., Watkins, D. N., Jair, K.-W., Schuebel, K. E., Markowitz, S. D., Chen, W. D., Pretlow, T. P., Yang, B., Akiyama, Y., van Engeland, M., Toyota, M., Tokino, T., Hinoda, Y., Imai, K., Herman, J. G., and Baylin, S. B. (2004) *Nat. Gen.* **36**, 417–422
- Rhee, C.-S., Sen, M., Lu, D., Wu, C., Leoni, L., Rubin, J., Corr, M., and Carson, D. A. (2002) *Oncogene* **21**, 6598–6605
- Nagahata, T., Shimada, T., Harada, A., Nagai, H., Onda, M., Yokoyama, S., Shiba, T., Jin, E., Kawanami, O., and Emi, M. (2003) *Cancer Sci.* **94**, 515–518
- Hedgepeth, C. M., Conrad, L. J., Zhang, J., Huang, H. C., Lee V. M., and Klein, P. S. (1997) *Dev. Biol.* **185**, 82–91
- Cohen, P., and Frame, S. (2001) *Nat. Rev. Mol. Cell Biol.* **2**, 769–776
- Ring, D. B., Johnson, K. W., Henriksen, E. J., Nuss, J. M., Goff, D., Kinnick, T. R., Ma, S. T., Reeder, J. W., Samuels, I., Slabiak, T., Wagman, A. S., Hammond, M. E., and Harrison, S. D. (2003) *Diabetes* **52**, 588–595
- Peifer, M., and Polakis, P. (2000) *Science* **287**, 1606–1609
- Shimamura, K., Hirano, S., McMahon, A. P., and Takeichi, M. (1994) *Development* **120**, 2225–2234
- Ikeya, M., Lee, S. M. K., Johnson, J. E., McMahon, A. P., and Takada, S. (1997) *Nature* **389**, 966–970
- Fuchs, S. Y., Spiegelman, V. S., and Kumar, K. G. S. (2004) *Oncogene* **23**, 2028–2036
- Dominguez, D., Montserrat-Sentis, B., Virgos-Soler, A., Guaita, S., Grueso, J., Porta, M., Puig, I., Baulida, J., Franci, C., and Garcia de Herreros, A. (2003) *Mol. Cell Biol.* **23**, 5078–5089
- Sabeh, F., Ota, I., Holmbeck, K., Birkedal-Hansen, H., Soloway, P., Balbin, M., Lopez-Otin, C., Shapiro, S., Inada, M., Krane, S., Allen, E., Chung, D., and Weiss, S. J. (2004) *J. Cell Biol.* **167**, 769–781
- Amit, S., Hatzubai, A., Birman, Y., Andersen, J. S., Ben-Shushan, E., Mann, M., Ben-Neriah, Y., and Alkalay, I. (2002) *Genes and Dev.* **16**, 1066–1076
- Liu, C., Li, Y., Semenov, M., Han, C., Baeg, G.-H., Tan, Y., Zhang, Z., Lin, X., and He, X. (2002) *Cell* **108**, 837–847
- Wang, Z., Vogelstein, B., and Kinzler, K. W. (2003) *Cancer Res.* **63**, 5234–5235
- Guaita, S., Puig, I., Franci, C., Garrido, M., Dominguez, D., Batlle, E., Sancho, E., Dedhar, S., De Herreros, A. G., and Baulida, J. (2002) *J. Biol. Chem.* **277**, 39209–39216
- Pinto, D., Gregorieff, A., Begthel, H., and Clevers, H. (2003) *Genes Dev.* **17**, 1709–1713
- Kuhnert, F., Davis, C. R., Wang, H.-T., Chu, P., Lee, M., Yuan, J., Nusse, R., and Kuo, C. J. (2004) *Proc. Natl. Acad. Sci. U. S. A.* **101**, 266–271
- Peinado, H., Quintanilla, M., and Cano, A. (2003) *J. Biol. Chem.* **278**, 21113–21123
- Tolwinski, N. S., and Wieschaus, E. (2004) *Trends Genet.* **20**, 177–181
- Aybar, M. J., Nieto, M. A., and Mayor, R. (2003) *Development* **130**, 483–494
- Zhurinsky, J., Shtutman, M., and Ben-Ze'ev, A. (2000) *J. Cell Sci.* **113**, 3127–3139
- Carver, E. A., Jiang, R., Lan, Y., Oram, K. F., and Gridley, T. (2001) *Mol. Cell Biol.* **21**, 8184–8188
- Zhou, B. P., Deng, J., Xia, W., Xu, J., Li, Y. M., Gunduz, M., and Hung, M.-C. (2004) *Nat. Cell Biol.* **6**, 931–940
- Schlessinger, K., and Hall, A. (2004) *Nat. Cell Biol.* **6**, 913–915
- Watanabe, N., Arai, H., Nishihara, Y., Taniguchi, M., Watanabe, N., Hunter, T., and Osada, H. (2004) *Proc. Natl. Acad. Sci. U. S. A.* **101**, 4419–4424
- Brennan, K. R., and Brown, A. M. C. (2004) *J. Mammary Gland Biol. Neoplasia* **9**, 119–131
- Hotary, K. B., Allen, E. D., Brooks, P. C., Datta, N. S., Long, M. W., and Weiss, S. J. (2003) *Cell* **114**, 33–45
- Miyoshi, A., Kitajima, Y., Sumi, K., Sato, K., Hagiwara, A., Koga, Y., and Miyazaki, K. (2004) *Brit. J. Cancer* **90**, 1265–1273
- Vega, S., Morales, A. V., Ocana, O. H., Valdes, F., Fabregat, I., and Nieto, M. A. (2004) *Genes Dev.* **18**, 1131–1143
- Spencer, E., Jiang, J., and Chen, Z. J. (1999) *Genes Dev.* **1**, 284–294
- Howe, L. R., Subbaramaiah, K., Chung, W. J., Dannenberg, A. J., and Brown, A. M. (1999) *Cancer Res.* **59**, 1572–1577